euspen's 20th International Conference & Exhibition, Geneva, CH, June 2020
www.euspen.eu

Criticalities of iterative calibration procedures for indentation testing machines in the nano-range

Giacomo Maculotti[1], Gianfranco Genta[1], Maurizio Galetto[1]

[1]*Department of Management and Production Engineering, Politecnico di Torino, Italy*

giacomo.maculotti@polito.it

Abstract
The modern manufacturing industry requires to achieve thorough multiscale mechanical characterisation to qualify processes and materials. Amongst the few available methods, Instrumented Indentation Test (IIT) outstands for its capabilities of estimating hardness, Young's modulus, stress-strains curve, creep and relaxation behaviour by means of a non-destructive procedure which analyses the force applied to the sample and the displacement of the indenter with respect to the sample surface continuously acquired during the application of a loading/unloading indentation cycle.
Traceability of the characterisation is ensured by calibration procedures described in the ISO 14577-2. In particular, the calibration of the frame compliance and the indenter area function are critical as they have been proven major contributor to the mechanical characterisation measurement uncertainty. Iterative methods, that do not require the indenter area function to be independently calibrated by means of high-resolution microscopes, e.g. AFM, are largely exploited in both academia and industry. Several calibration recipes are available according to the standard and reference literature. These include different reference materials, algorithms, and testing procedures, in terms of force range and number of tests. However, literature lacks detailed works aimed at reporting the performances of the several available methods combining the possible parameters admissible for the standard. Furthermore, approaches for estimating the measurement uncertainty of this calibration are undefined in both literature and the standard.
This work, exploiting a Monte Carlo approach for evaluating calibration uncertainty, discusses the results of the comparison of these calibration methods in the nano-range. Shortcomings of the standard due to the effect of calibration materials and algorithms are highlighted and discussed.

Instrumented nano-indentation test, calibration method, frame compliance, indenter area

1. Introduction

Amongst mechanical characterisation methods, IIT is a depth-sensing indentation technique that requires limited sample preparation. It received actual interest in the research and industrial community since late '80s because it allows characterisation at nano-range overcoming limits set by optical instrument resolution [1]. IIT requires to indent a material by means of a loading-unloading cycle, throughout which the applied force, F, and the indenter displacement, h, are measured by devoted transducers. Mechanical characterisation can be achieved by analysing the loading-unloading cycle, when expressed in terms of applied force as function of indenter displacement, i.e. $F(h)$, that is referred to as indentation curve (IC), which Fig. 1 shows. IIT can effectively provide, as an at most semi-destructive test, thorough mechanical characterisation in terms of hardness, estimate of Young's modulus, creep and relaxation behaviour of the material [2,3], the map of mechanical properties of the microstructure of metallic materials by distinguishing amongst different phases and precipitates [4,5], and the estimate of characteristic dimension of microstructure [6]. Therefore, it is attractive for online quality control and rapid set-up of manufacturing processes. Consequently, given the widespread interest in this technique, it is standardised by the ISO 14577, latest reissued in 2015.

Measured data during the indentation cycle require to be corrected to account for some measurement errors. In particular, h is affected by a zero error h_0, by the elastic deformation of the sample reference surface which dependes on the indenter shape: $\varepsilon F/S$ (where S is the contact stiffness, i.e. the sample stiffness, and ε is a shape factor depending on the indenter type, e.g. for Berkovich indenter it is 0.75), and by the elastic deformation of the indentation testing machine: C_f (i.e. the frame compliance) [7]. When these contributions are considered, the corrected displacement, h_c, results according to:

$$h_c = h - h_0 - \varepsilon\frac{F}{S} - C_f F \tag{1}$$

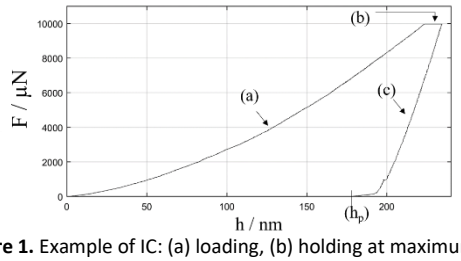

Figure 1. Example of IC: (a) loading, (b) holding at maximum load necessary for creep compensation, (c) unloading and the residual indentation h_p.

The contact stiffness can be evaluated, by modelling the indenter-sample system as a couple of ideal springs representing for the testing machine, with a compliance C_f, and the sample, with stiffness S. Due to the modelling and by their definitions [1,2], it follows:

$$C_{tot} = \frac{1}{S_m} = \left(\left.\frac{\partial F}{\partial h}\right|_{h_{max}}\right)^{-1} = C_f + \frac{1}{S} \tag{2.1}$$

$$S = \left.\frac{\partial F}{\partial h_c}\right|_{h_{c,max}} \quad (2.2)$$

where C_{tot} is the total compliance of the system and can be retrieved from the measured raw data as the inverse of the measured, i.e. total, stiffness, S_m.

In order to evaluate the S_m, ISO 14577-1:2015 [3] requires the unloading curve to be fitted according to a pre-defined mathematical model, which has to be differentiated and computed in the point corresponding to the onset of unloading. In particular, the power law method (PL) [2] provides best results, amongst the standard alternatives [8]. It describes the bulk of the unloading curve as:

$$F = B\left(h - h_p\right)^m \quad (3)$$

where the terms B and m are estimated by least squares fitting to the experimental data within an interval usually between 98% and 20% of the maximum force reached during the cycle, F_{max}. PL provides unbiased results, which, though, are characterised by a high measurement uncertainty [8]. Moreover, this procedure estimates the derivative of a curve from its primitive fitting, which, even though minimises the sum of squared residuals, does not guarantee any properties of the derivative. This is critical because S, according to Eq. (2.2), is the derivative of Eq. (3) at the maximum penetration depth, h_{max}. Thus, literature suggested a methodology, hereafter referred to as DM (i.e. Derivative Method), based on the direct derivative evaluation to provide a metrological evaluation of S consistent with its definition [9].

To achieve the mechanical characterisation, the contact area surface needs to be estimated; this can be retrieved directly from continuous recording of h during the indentation cycle, if the area shape function, $A_p(h)$, is known. $A_p(h)$ describes the projection on the tested surface of the lateral surface of the indenter in contact with the sample as a function of the distance from its apex; for the most typical case of an ideal modified Berkovich indenter, i.e. a tetrahedron with dihedral angle of 130.56°, it is $A_p(h) = 24.5 \cdot h^2$ and $\varepsilon = 0.75$ [3]. However, due to deviations from ideal geometry, which are mostly due to blunting and offset of the tip and wear, $A_p(h)$ results in a more general quadratic function [10,11], which can be written in both terms of raw (h) or corrected (h_c) displacement:

$$A_p(h) = a_2h^2 + a_1h + a_0 \quad (4)$$

The indentation hardness, H_{IT}, and the indentation modulus, E_{IT} are some of the several characterisation results of IIT. The latter provides an estimate of the tested material elastic modulus, by means of a non-destructive procedure. E_{IT} depends on IIT test results and the mechanical properties of the indenter, i.e. its Poisson's, ν_i, and Young's modulus, E_i, and the Poisson's modulus of the tested material, ν_s:

$$H_{IT} = \frac{F_{max}}{A_p(h_{c,max})} \quad (5.1)$$

$$E_{IT} = \frac{1-\nu_s^2}{\frac{2\sqrt{A_p(h_{c,max})}}{S\sqrt{\pi}} - \frac{1-\nu_i^2}{E_i}} \quad (5.2)$$

The accuracy and precision of material characterisation is core to be achieved; therefore, careful calibration of testing machine according to ISO 14577-2:2015 [10] is necessary to guarantee traceability and to establish uncertainty contribution to final results. Barbato et al. [8] demonstrated that major contributors to measurement uncertainty of the indentation modulus, in the nano-range, are the C_f and the parameters of $A_p(h)$. Annex D of ISO 14577-2:2015 introduces five methods for their calibration. Methods no. 1, 3 and 5 allow to calibrate $A_p(h)$ parameters by means of a measurement of the indentation tip by a metrological AFM and to subsequently calibrate C_f. These, despite yielding a smaller calibration uncertainty are more expensive [11]; therefore, methods no. 2 and 4 are often preferred. They rely upon an iterative procedure outlined to achieve the calibration, by exploiting relationships that can be inferred from IC without the need of the AFM calibration of the $A_p(h)$. Although the widespread adoption of method no. 2 and no. 4, ISO 14577-2:2015 does not suggest any good practice to perform such calibrations; moreover, literature [11,12] and practices of research laboratories or testing machine manufacturers show quite a variety of solutions, whose compliancy is not reported.

This work aims at comparing the calibration results of C_f and $A_p(h)$, and their effect on material characterisation in the nano-range, when methods no. 2 and 4 are adopted. The investigation will be based on a Monte Carlo approach for evaluating calibration uncertainty; the effect of calibration materials and algorithms will be discussed. The paper is structured as follows. Section 2 describes the calibration methods, Section 3 describes the experimental methodology, Section 4 discusses the main results, and Section 5 eventually concludes the findings.

2. Calibration procedure

This section discusses the two methods outlined in ISO 14577-2:2015, which will be investigated in the present work. As mentioned in the previous section, the overall stiffness is measured from raw data, according to its definition, as in Eq. (2.1). Moreover, considering the definition of reduced modulus E_r in Eq. (6) and combining it with Eq. (2.1), the linear relationship in Eq. (7) between $1/S_m$ and $1/\sqrt{A_p(h_{c,max})}$ results, whose intercept is the C_f and from which Eq. (8) follows.

$$1/E_r = \frac{1-\nu_s^2}{E_s} + \frac{1-\nu_i^2}{E_i} = \frac{2}{\sqrt{\pi}}\frac{\sqrt{A_p(h_{c,max})}}{S} \quad (6)$$

$$1/S_m = C_{tot} = C_f + \frac{\sqrt{\pi}}{2E_r\sqrt{A_p(h_{c,max})}} \quad (7)$$

$$A_p\left(h_{c,max}\right) = \frac{\pi}{4E_r^2\left(C_{tot} - C_f\right)^2} \quad (8)$$

Thus, an iterative procedure, whose workflow is shown in Fig. 2, is outlined to calibrate parameters and achieve convergence of the values obtained [10]. It requires I indentations, $I \geq 5$, to be performed over a load range which is representative for the application field of the instrument [10]. The procedure holds fixed ε and E_r, which enables for a calibration. Initialisation of the problem is performed in step 2 and 3 assuming ideal conditions, i.e. infinitely stiff testing machine and ideal indenter geometry. In Fig. 2, $\boldsymbol{F_{max}}$, $\boldsymbol{S_m}$, $\boldsymbol{h_{max}}$, $\boldsymbol{h_{c,max}}$, $\boldsymbol{h_0}$ and $\boldsymbol{A_p(h_{c,max})}$ are column vectors built, exploiting $\boldsymbol{F_{max}}$ as an example, as:

$$\boldsymbol{F_{max}} = \left\{\boldsymbol{F_{max,i,j}}\right\} \quad (9)$$

where i counts the load range levels at which J replicated indentations are performed, i ranges from 1 to I, j from 1 to J. Moreover, arrays are sorted so that $\boldsymbol{F_{max,w,\cdot}} > \boldsymbol{F_{max,w+1,\cdot}}$, with w ranging from 1 to I-1.

Custom script was implemented in *MATLAB R2018b*, convergence was achieved as the variation of mean values of

calibrated parameter from cycle k and k-1 is smaller than 0.1% and furtherly checked on root mean square error stabilisation.

The standard includes two versions of this iterative method: method no. 2 and method no. 4. The former prescribes the calibration to be performed according to workflow presented in Fig. 2 by indenting a single sample, which must have a low E, e.g. fused silica (SiO_2) or monocrystalline aluminium (Al), to allow the calibration of $A_p(h)$ parameters even at low forces. Problem initialisation is performed by exploiting data from the indentations at the two higher loads, i.e. $i \in \{1,2\}$; subsequent iterations exploits all collected data. The latter prescribes to indent two samples of different materials: a material with higher E, e.g. tungsten (W), shall be considered to calibrate C_f, whilst a material with lower E, e.g. SiO_2 or monocrystalline Al, enables the calibration of $A_p(h)$ parameters. Therefore, steps 1 to 4, and consequently 7, have to be performed considering data from tungsten indentations, whilst steps 5 and 6, which calibrate shape function parameters, require data from the material with lower E. This method, by decoupling calibration and material, guarantees faster convergence [11] and allows the initialisation to be performed considering all data, i.e. $i \in \{1, \ldots, I\}$, on the material with higher modulus.

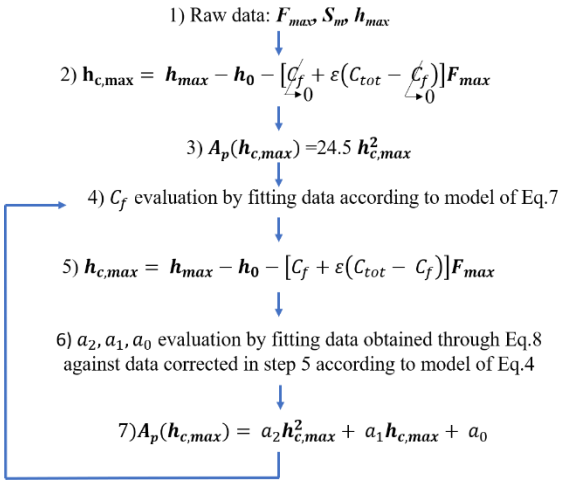

Figure 2. *Workflow of the calibration iterative procedure.*

3. Methodology

3.1. Experimental setup

A Triboindenter TI 950 by Hysitron, hosted in the facilities of the Istituto Italiano di Tecnologia and equipped with a modified Berkovich indenter (E_i = 1140 GPa, ν_i = 0.07 and ε = 0.75), was calibrated on calibrated samples, whose characteristics are summarised in Table 1. The testing equipment features a force-displacement three-plate capacitive transducer with resolution and noise floor, respectively, of 1 nN and 100 nN, on force, and of 0.04 nm and 0.2 nm, on displacement. This platform allows to assume h_0 = 0.

Table 1 Calibrated materials characteristics.

Material	Calibration	E / GPa	ν
SiO_2	NPL	73.3 ± 0.6	0.161 ± 0.003
W	NPL	413.0 ± 2.8	0.281 ± 0.003

According to literature [10–12] the experimental plan, summarised in Table 2, was outlined to properly cater for different degrees of freedom:

- calibration method: no. 2 (M2) and no. 4 (M4) from ISO 14577-2:2015,
- contact stiffness evaluation method: PL [2] and DM [9],
- material: SiO_2 and on the couple of W and SiO_2,
- load range: from 1 mN to 10 mN and from 3 mN to 10 mN,
- range sampling conditions: five evenly spaced loads with ten replicated measurements ($10r$) and fifty evenly spaced loads with no replication providing a denser sampling (DS).

Tungsten is always tested on the 1 mN to 10 mN range to provide C_f calibration in the whole operating range of the machine. On the other hand, provided the known greater signal to noise ratio at low loads, the reduced range from 3 mN to 10 mN has been introduced for SiO_2. Force controlled tests, according to manufacturer best practices, feature a loading curve of 9 s, a hold phase of 2 s and an unloading phase of 5 s.

Results will be provided in terms of C_f and, considering an indentation performed with the same force controlled cycle with a maximum force of 10 mN on SiO_2, of H_{IT} and E_{IT}.

Table 2 Experimental plan implemented to assess performances of calibration methods.

Material	M2				M4 with W at (1-10) mN			
	PL		DM		PL		DM	
SiO_2 (1-10) mN	10r	DS	10r	DS	10r	DS	10r	DS
SiO_2 (3-10) mN	10r	DS	10r	DS	10r	DS	10r	DS

3.2. Monte Carlo setup and uncertainty estimation

In order to provide a comparison of calibration methods performances, calibration results must be compared in terms of mean value and measurement uncertainty. However, the iterative algorithms, which enable for the calibration to be performed, hamper the implementation of simple closed formulae, defined in JCGM 100, that allows to compose uncertainty contributions [13]. Thus, this work, to assess calibration methods performances within a metrological framework, exploits a Monte Carlo method (MCM) to estimate the ralated uncertainties. A MCM was set up considering the influence factors with the distributional hypotheses summarised in Fig. 3. Experimental sources, calibrated sources and results of fitting are assumed to distribute according to normal distributions, tabular sources according to uniform distribution; the iterative method introduces as influence factors the output themselves.

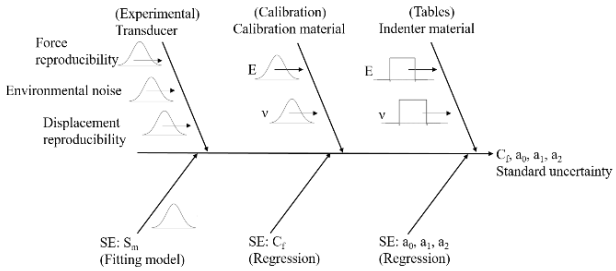

Figure 3. Ishikawa diagram for influencing factors of standard uncertainty of calibration methods results.

According to JCGM 101 [14], 10000 iterations are performed, distribution evaluated so that results to compare calibration methods' performances will be provided in terms of mean and expanded uncertainty at 95% confidence level.

4. Results discussion

Referring to the experimental plan of Table 2, 16 configurations are considered. Results of the calibration of C_f are shown in Fig. 4, where error bars represent uncertainty intervals evaluated exploiting a MCM, see Section 3.2.

Method no. 2 has in general worst performances in both terms of accuracy and precision than method no. 4: mean estimate shows greater variability between different cases of the former with respect to the latter, and in some cases distribution is not symmetrical. This suggests a lack of robustness of method no. 2

to measurement disturbances, which are more likely to happen when lower loads are included, i.e. (1-10) mN range, or when replicated measurements are not included, i.e. *DS* case. The decoupling of C_f and $A_p(h)$ parameters calibration in method no. 4 allows to relieve the effect of those issues. Provided limitations of method no. 2, the adoption of several load points, i.e. load range sampling case *DS*, does not provide any advantage in calibration accuracy but worsen the precision. Similarly, a wider range coupled with a more robust calibration method, i.e. *[M4; (1-10) mN]*, provides more precise results than a narrower one. A wider range also guarantees unbiased estimation of C_f, as shown in Figure 5.

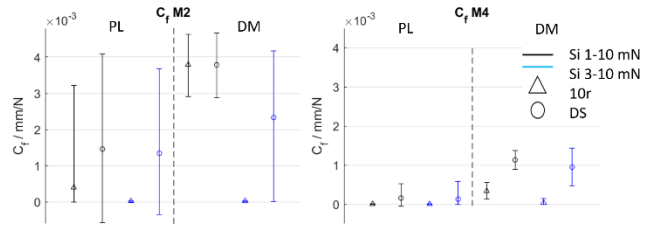

Figure 4. Performance comparison of calibration method for C_f.

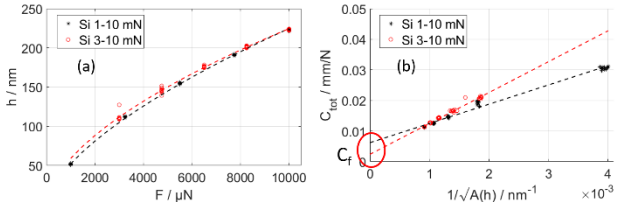

Figure 5. (a) $h(F)$, see Eq.(3): despite the consistency in h measurement at F=1 mN in data set (1-10) mN and the expected value from (3-10) mN, (b) different data spread biases the estimate of C_f, i.e. the intercept.

These behaviours of the calibration methods depending on the investigated degrees of freedom reflect on results of characterisation. Figures 6 and 7 show estimated E_{IT} and H_{IT} for the corresponding calibration for a measurement on SiO_2 at 10 mN. Scaling the analysis from C_f to H_{IT} and E_{IT}, the difference in accuracy amongst considered cases becomes less significant. However, precision becomes critical and shows that results are sometimes not compliant with calibrated value of H_{IT}, which can be explained considering that the calibration methods only require information of E_r. Also, the adoption of DM yields more precise results than PL, consistently to the method definition, when noise content is limited.

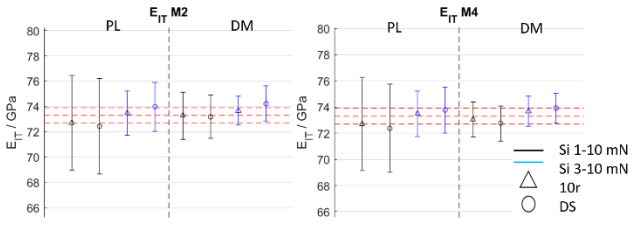

Figure 6. Calibration method effect on E_{IT}. Red lines are reference from calibration certificate.

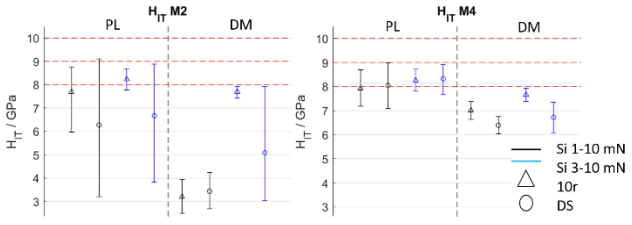

Figure 7. Calibration method effect on H_{IT}. Red lines are reference from literature.

5. Conclusions

Given the characterisation capabilities of instrumented indentation test, the accuracy and precision of the results are core to guarantee reliable information. This work compared performances of different calibration recipes applied to standard iterative calibration methods for frame compliance and area shape function parameters. Results showed the lack of robustness and unsatisfactory dependence on calibration setup of accuracy and precision of both calibration and characterisation of current standard calibration methods. Improvement of the calibration may be achieved either by exploiting AFM, although with high related costs, or by the development of improved approaches. The authors are studying a single-step procedure that is expected to obtain advantages in terms of implementation and measurement uncertainty of both calibration and mechanical characterisation as compared to the state of the art.

Acknowledgements

This work has been partially supported by "Ministero dell'Istruzione, dell'Università e della Ricerca". Award "TESUN-83486178370409 finanziamento dipartimenti di eccellenza CAP. 1694 TIT. 232 ART. 6"

References

[1] Lucca D A, Herrmann K, Klopfstein M J 2010 Nanoindentation: Measuring methods and applications *CIRP Ann. – Manuf. Technol.* **59** 803–19.

[2] Oliver W C, Pharr G M 1992 An improved technique for determining hardness and elastic modulus using load and displacement sensing indentation experiments *J. Mater Res* **1**(4) 601-609.

[3] ISO 14577-1:2015 Metallic materials - Instrumented indentation test for hardness and materials parameters - Part 1: Test method. ISO, Genève.

[4] Engqvist H, Wiklund U 2000 Mapping of mechanical properties of WC–Co using nanoindentation *Tribol. Lett.* **8** 147–52.

[5] Maculotti G, Senin N, Oyelola O, Galetto M, Clare A, Leach R 2019 Multi-sensor data fusion for the characterisation of laser cladded cermet coatings *Conf. Proc. of 19th Int Conf Exhib EUSPEN* 260–3.

[6] Hou X, Jennett N M, Parlinska-Wojtan M 2013 Exploiting interactions between structure size and indentation size effects to determine the characteristic dimension of nano-structured materials by indentation *J. Phys. D Appl. Phys.* **46**(26) 265301.

[7] Cagliero R, Barbato G, Maizza G, Genta G 2015 Measurement of elastic modulus by instrumented indentation in the macro-range: Uncertainty evaluation *Int. J. Mech. Sci.* **101–102** 161–9.

[8] Barbato G, Genta G, Cagliero R, Galetto M, Klopfstein M J, Lucca D A, Levi R 2017 Uncertainty evaluation of indentation modulus in the nano-range: Contact stiffness contribution *CIRP Ann. – Manuf. Technol.* **66** 495–8.

[9] Maculotti G, Genta G, Lorusso M, Pavese M, Ugues D, Galetto M 2018 Instrumented Indentation Test: Contact Stiffness Evaluation in the Nano-range *Nanomanufacturing Metrol.* **2**(1) 16–25.

[10] ISO 14577-2:2015 Metallic materials - Instrumented indentation test for hardness and materials parameters - Part 2: Verification and calibration of testing machines. ISO, Genève.

[11] Herrmann K, Jennet N M, Wegener W, Meneve J, Hasche K, Seeman R 2000 Progress in determination of the area function of indenters used for nanoindentation *Thin. Solid. Films* **377–378** 394–400.

[12] Meneve J L, Smith J F, Jennett N M, Saunders S R J 1996 Surface mechanical property testing by depth sensing indentation *Appl. Surf. Sci.* **100–101** 64–8.

[13] JCGM 100: 2008 Evaluation of measurement data — Guide to the expression of uncertainty in measurement (GUM). JCGM, Sèvres (France).

[14] JCGM 101:2008 Evaluation of measurement data -- Supplement 1 to the "Guide to the expression of uncertainty in measurement" -- Propagation of distributions using a Monte Carlo method. JCGM, Sèvres (France).